applied sciences

MDPI

Article

The Determination of Combustion for Different Pellets Based on Ostwald Diagrams in a Domestic Stove under Experimental Conditions

Juan Félix González [1], Andrés Álvarez Murillo [2], Diego Díaz García [1] and Sergio Nogales-Delgado [1,*]

[1] Department of Applied Physics, University of Extremadura, Avda. De Elvas, s/n, 06006 Badajoz, Spain; jfelixgg@unex.es (J.F.G.); ddiazm@alumnos.unex.es (D.D.G.)
[2] Department of Teaching of Experimental Sciences and Mathematics, University of Extremadura, Avda. De Elvas s/n, 06006 Badajoz, Spain; andalvarez@unex.es
* Correspondence: senogalesd@unex.es

Featured Application: A thorough study about the optimization of a real biomass stove through the use of different fuels was carried out to determine the quality of exhaust gases.

Abstract: The global energy scenario is becoming a vital aspect of the sustainable economic development of regions and countries. Current changes in energy production, mainly due to scarcity and geopolitical factors, have proven the need for changes in energy distribution towards a lower energy dependence. Moreover, a considerable amount of biomass waste is generated in many regions, because of agro-industrial activities, whose management could contribute to energy production. The aim of this work was to study the optimization of the combustion process in a biomass stove by using different raw materials as fuels, such as pine, poplar, and plum tree pellets. For that purpose, power, excess air, and biomass content were optimized, among other parameters, and exhaust gases were analyzed with a Testo 335 analyzer, while temperatures were recorded with temperature probes. In conclusion, high yields were found for the optimized parameters of the studied biomass products (ranging from 91.1% for poplar pellets to 92.34% for pine pellets), making these three biomass fuels suitable for combustion in the abovementioned stove. Also, increasing biomass flow by 25% in the stove contributed to a higher efficiency of the process, especially in the case of plum tree pellets.

Keywords: combustion; biomass; optimization; biomass; pine; poplar; plum tree; exhaust gas analysis

Citation: González, J.F.; Álvarez Murillo, A.; Díaz García, D.; Nogales-Delgado, S. The Determination of Combustion for Different Pellets Based on Ostwald Diagrams in a Domestic Stove under Experimental Conditions. *Appl. Sci.* **2023**, *13*, 12007. https://doi.org/10.3390/app132112007

Received: 22 September 2023
Revised: 27 October 2023
Accepted: 30 October 2023
Published: 3 November 2023

1. Introduction

1.1. Global Energy Scenario

The global energy scenario is one of the most challenging issues when it comes to the global development of a country. The current oscillations in energy production, due to many factors, such as geopolitics or international relations, have pointed out, in the cases of many countries (especially smaller or less powerful ones, which are usually more dependent and vulnerable compared to world powers, such as China or the USA [1]), the need for modifications in energy patterns towards a lower energy dependency, which would imply a boost for their economies and industrial activities [2], possibly reducing the influence of international oil companies (IOCs) in energy transition, as in the case of Europe [3]. Notably, the possibility for many countries to become "prosumer actors" through a green transition could reduce any form of geopolitical concern [4]. For instance, in the case of Europe (according to recent studies), it is vital to replace energy imports with domestic energy production, in order to reduce energy dependency. If import substitution takes place using domestic renewable energy sources, additional positive effects could be found in terms of energy dependency and security, as well as sustainable development [5].

Additionally, there is an increasing concern (at both the national and international levels) about environmental issues such as climate change, with greenhouse gas emissions being among the most worrying aspects related to industrial activities and energy consumption. As a result, international organizations, such as the United Nations, have been fostering the Sustainable Development Goals (SDGs), for which the implementation of specific steps to promote sustainable economic and energy growth (especially in the cases of developing countries) have an essential role, promoting concepts such as green chemistry, circular economy, or atom efficiency, among others, in order to maintain the environmental quality of soil, water, and air [6].

Specifically, the use of biomass could play an important role in the implementation of these SDGs or similar biomass-, bioprocessing-, or other bio-based product policies, implying, in many cases, the valorization of waste with difficult environmental management, through its energy use at local and industrial levels, and possibly contributing to bioeconomic strategies (of which many are still not completely coherent with common bioeconomic objectives), thus becoming an interesting resource through which to improve the use of marginal lands that can alleviate resource competition and soil deterioration [7].

Additionally, the data included in Figure 1 support the abovementioned reasoning. Thus, if worldwide pellet production is considered (Figure 1a), an exponential increase can be observed over the last two decades, which points out the commercialization of biomass at the global level. Also, in the case of Europe, there was a steady increase in solid biomass primary energy production, from around 50 million tons of oil equivalent in 2000 to about 100 million tons in 2021 (that is, production doubled). This fact could imply an increase in the implementation of biomass power plants. For instance, regarding Germany (Figure 1c), there was a 16% increase in the use of biomass power plants in the last decade, pointing out the commitment of this country to renewable energies, including biomass. Last but not least, the role of biomass in some developing regions or countries could be important, as shown in Figure 1d, in the case of electricity generation from biomass and waste in Africa. As observed, electricity generation doubled in two decades, demonstrating this energy source as an interesting way to contribute, among other renewable energies, to the sustainable development of Africa. Indeed, interesting work has been carried out regarding the use of local biomass in boilers, as in the case of Cameroon [8].

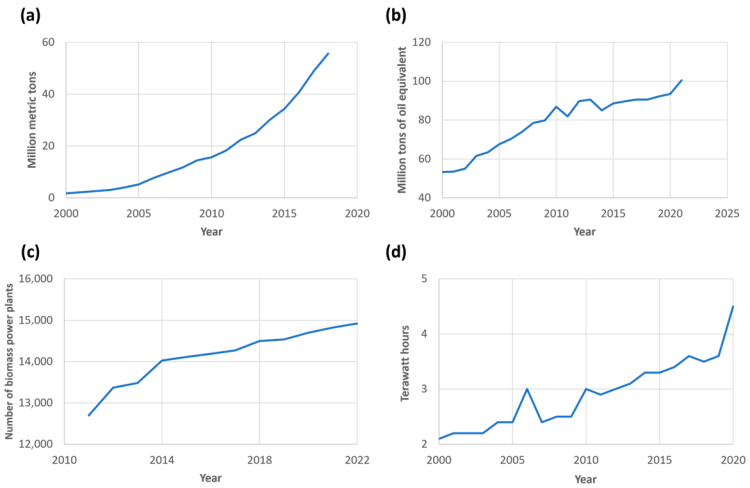

Figure 1. Different trends regarding biomass within the last two decades: (**a**) global wood pellet production (source: [9]); (**b**) solid biomass primary energy production in Europe (source: [10]); (**c**) number of biomass power plants in Germany (source: [11]); (**d**) electricity generation (in terawatt hours) from biomass and waste in Africa (source: [12]).

These data support the contribution of this energy source to sustainable development in general, increasing the energy independence of countries and regions, and managing some agricultural waste products, thus improving their valorization. In general, biomass

energy use is devoted to local consumption, that is, many countries, such as Finland or Sweden, consume almost all of the biomass energy produced by themselves [13,14]. Nevertheless, there are other countries where biomass energy production exceeds its consumption, as in the case of Portugal [15], whereas the opposite also takes place, with a higher consumption compared to biomass energy production (for instance, in Italy) [16]. In any case, these differences are not significant, showing relatively similar biomass energy production and consumption.

Concerning Spain (whose biomass energy production/consumption ratio is also balanced, according to recent data [17]), and specifically in the Extremadura region, a considerable amount of biomass waste is continuously generated due to diverse agro-industrial activities. Nevertheless, these waste products present high potential for energy generation (including barks, husks, corncobs, etc.), which represents a great opportunity for the implementation of circular economy or green chemistry policies [18,19]. Conventionally, these waste products are used for direct combustion and subsequent energy generation through steam cycles. In that sense, combustion optimization (for instance, that taking place in a stove) is essential to making this process energy and economically feasible at both the user and industrial levels.

1.2. Combustion: Foundations and Optimization

Combustion is a chemical reaction in which oxidizing air is combined with oxidable elements together in a combustible substance. Through this chemical reaction, energy is released as heat. The chemical species that are obtained are considered reaction products, exhaust gas, or combustion gas. For this purpose, pure oxygen is not usually used, whereas oxidizing gas is normally employed (for instance, air). Thus, there are different kinds of combustion, including complete combustion (in which the combustible is completely oxidized), neutral combustion (a complete combustion in which stoichiometric oxygen is used), and incomplete combustion (in which the combustible is not completely oxidized).

Moreover, the heating value of a fuel is the heat released in a complete combustion for one unit of fuel. Thus, the heating value can be determined as a high heating value (HHV) or a low heating value (LHV), depending on the consideration of steam condensation due to combustion or water content in the fuel. Thus, the only difference between HHV and LHV is the condensation heat of steam (produced during combustion or included in the fuel). As a consequence, this parameter is extremely important in this context, as the use of fuels with specific heating values will determine the efficiency of combustion processes in stoves.

Combustion facilities, such as those including stoves, are usually designed to obtain the highest yield possible, that is, an optimum yield, in order to make combustion as efficient as possible. For that purpose, energy loss should be minimal. Thus, loss due to sensible heat, or solid and gaseous non-burnt products, can be reduced if the excess air coefficient (n, included in Equation (1)) is adjusted, which is difficult to achieve in a specific facility.

$$n = \frac{air_r}{air_t} \quad (1)$$

where air_r is the real air in the facility and air_t is the theoretical air that should be provided. Thus, loss due to sensible heat is due to the fact that a percentage of the generated heat during combustion is not useful, as the exhaust gases evolve at higher temperatures compared to their behaviors at the ambient temperature. Considering the exhaust gases (P_s) as a mixture of ideal gases, this loss can be assessed according to Equation (2), as follows:

$$P_s = \Delta H = H_h - H_a = m_h C_{ph}(T_h - T_a) = V_h \rho_h C_{ph}(T_h - T_a) \quad (2)$$

where:

- h_h—h_a represents the enthalpy change in the exhaust gases.
- m_h is the exhaust flow.
- C_{ph} is the average specific heat of the exhaust gases.

- T_h—T_a are the inlet and outlet temperature, respectively, of the exhaust gases and the air.
- V_h and ρ_h are the total volume generated and the exhaust gas density, respectively.

Thus, loss could be avoided if $V_h = 0$ or $T_h = T_a$. The way to reduce these losses is to decrease the outlet temperature and the total volume of the exhaust gases. In the first case, heat recovery systems are used for the exhaust gases to decrease T_h, or for air heaters to increase T_a. Also, superheaters or reheaters can be used for this purpose. The total exhaust gas volume reduction can thus be achieved by reducing excess air. In fact, this loss is minimal if the minimum air necessary for the combustion of a specific combustible is used.

Losses due to non-combusted gas occur on account of the presence of combustible gas, mainly CO. An LHV in a solid fuel can be calculated, according to its elemental analysis (dry basis), through Equation (3), as follows:

$$\mathrm{LHV} = 8100\mathrm{P_C} + 34,400\mathrm{P'_{H_2}} + 2500\mathrm{P_S} - 5400\mathrm{P_{H_2}} \quad (3)$$

where P_C is the percentage, by weight, of carbon obtained in the ultimate analysis, P'_{H_2} is the hydrogen available to be burned, P_{H_2} is the percentage, by weight, of hydrogen obtained in the ultimate analysis, and P_S is the percentage, by weight, of sulfur obtained in the ultimate analysis; all of these values are expressed in kg of each element per kg of fuel. If the total combustion of carbon takes place, the following reaction occurs (see Equation (4)):

$$\mathrm{C} + \mathrm{O_2} \rightarrow \mathrm{CO_2} + 8100\ \mathrm{Kcal/kg} \quad (4)$$

If combustion is incomplete (obtaining CO), the P_C value would be $P_C \cdot (1 - x)$, and the following reaction takes place (Equation (5)):

$$\mathrm{C} + \frac{1}{2}\mathrm{O_2} \rightarrow \mathrm{CO} + 2430\ \mathrm{Kcal/kg} \quad (5)$$

where x is the burned gas ratio, $(1 - x)$ is the unburned gas ratio (which is evolved), $P'_{H_2} = P_{H_2} - P_{O_2}/8$ (for wet basis), and $P'_{H_2} = P_{H_2}$ for dry basis. Thus, according to Equation (6):

$$\mathrm{x} = \frac{\nu_{CO_2}}{\nu_{CO} + \nu_{CO_2}} \quad (6)$$

the loss due to unburned gas (P_{ub}) would be obtained according to Equation (7), as follows:

$$\mathrm{P_{ub}(CO)} = 8100\ \mathrm{P_C} - [8100\mathrm{P_C x} + 2430\mathrm{P_C}(1 - \mathrm{x})] = 5670\mathrm{P_C}(1 - \mathrm{x}) \quad (7)$$

where P_C is the amount of carbon in the utilized biomass. From the previous equation, it can be inferred that the lower the value of x, that is, the more incomplete the combustion, the higher the loss will be. Therefore, this loss will be avoided when carrying out a complete combustion. This can be achieved by pulverizing the fuel, provoking turbulence to increase the contact between the oxidizing agent and the fuel, providing a suitable excess air coefficient, increasing the heat in the stove, or increasing the combustion time.

Therefore, concerning these losses, an optimum excess air coefficient is needed to contribute to a maximum yield, as can be observed in Figure 2. The indirect method through which to determine the yield of the process is based on the calculation of all losses that take place in the oven through Equation (8), as follows:

$$\eta = 1 - \frac{\sum \mathrm{P}}{\mathrm{LHV}} \quad (8)$$

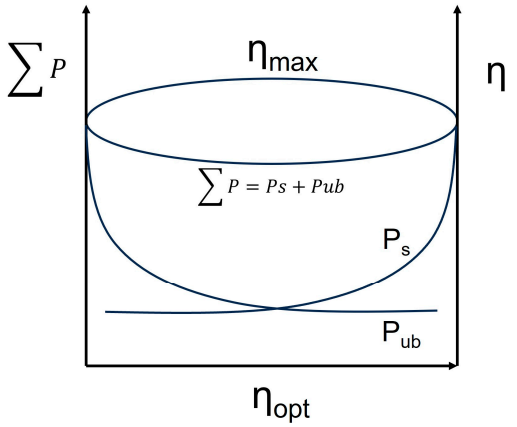

Figure 2. Loss, yield, and their relationships to the excess air coefficient.

The graphical representation of loss through sensitive and latent enthalpy presents a disadvantage, that is, the impossibility of finding a general mathematical expression that correlates both losses according to excess air (n). For this reason, the only reliable way to represent these equations is through experimental sampling of each combustion facility, in order to test different excess air ratios.

1.3. Ostwald Diagram: Theoretical Foundations

In order to optimize combustion processes, a mathematical tool (developed by Wilhelm Ostwald and used in the literature for some time to determine the performance of biomass facilities [20]) will be used with the fuel parameters obtained for each combustion stage. If the flue gas composition is known, in percentage, it is possible to represent the stage of the process. Thus, in Figure 3, an example of an Ostwald diagram can be observed.

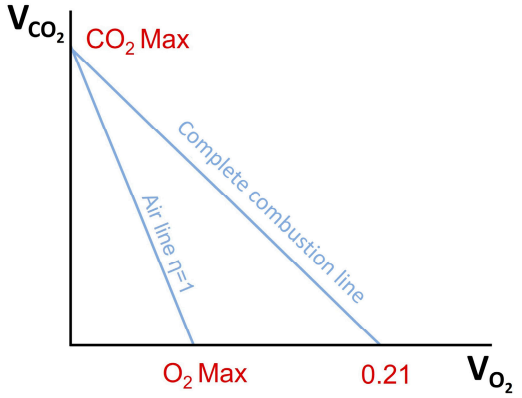

Figure 3. Example of an Ostwald diagram.

Thus, the two catheti, or legs, represent the values of V_{CO_2} and V_{O_2} in the exhaust gases, and the hypotenuse represents the complete combustion line. The triangle is divided, in turn, by the so-called air line, into two parts: one representing the incomplete combustion points due to the lack of air (triangle corresponding to the ordinate–abscissa–air lines), and another one representing the incomplete combustion due to excess air (triangle corresponding to the air–abscissa–complete combustion lines).

Regarding the complete combustion line, it is the geometric line corresponding to V_{CO_2} and V_{O_2}, that is, corresponding to complete combustion (see Equation (9)).

$$V_{O_2} + V_{CO_2}\left(1 + 0.79\frac{3P'_{H_2}}{P_C}\right) = 0.21 \quad (9)$$

Thus, this line has a value, at the abscissa axis, of 0.21, whereas its value at the ordinate axis is CO_2 max. This first point, CO_2 max, $V_{O_2} = 0$ (which corresponds to combustion in the absence of oxygen, that is, a neutral combustion with $\eta = 1$), depends on the kind of fuel (its composition), whereas the value at the abscissa axis is always 0.21, regardless of the fuel used and, therefore, it is common to every Ostwald diagram. Concerning the air line, it is the line whose excess air coefficient equals one. For its representation, previous equations are required. If n = 1 and CO_2 max and O_2 max are calculated, the intersection points with the abscissa and ordinate axis are obtained (Equations (10) and (11)) as follows:

$$V_{CO_2} = \frac{\frac{P_C}{12}x}{\frac{100n-21}{21}\left(\frac{P_C}{12} + \frac{P'_{H_2}}{4}\right) + \frac{P_C\left(1+\frac{1-x}{2}\right)}{12}} \quad (10)$$

$$V_{O_2} = \frac{\left(\frac{P_C}{12} + \frac{P'_{H_2}}{4}\right)(\eta - 1) + \frac{1}{2}\frac{P_C}{12}(1-x)}{\frac{100n-21}{21}\left(\frac{P_C}{12} + \frac{P'_{H_2}}{4}\right) + \frac{P_C\left(1+\frac{1-x}{2}\right)}{12}} \quad (11)$$

Line n = 1 divides the triangle into two parts, the one on the left corresponding to incomplete combustion due to the lack of air, and the one on the right corresponding to incomplete combustion due to excess air. It should be noted that another property of line $\eta = 1$, as $V_{CO} = 2V_{O_2}$, if the V_{O_2} values are correlated to this line, the V_{CO} scale is obtained by multiplying these values by two, which is a scale that can be projected over an additional axis, perpendicular to the hypotenuse of the triangle. Regarding the lines obtained when V_{CO} is constant, even though these are theoretical curves, they can be considered as straight lines, as the difference is negligible. Thus, these lines are obtained by drawing parallel lines to the hypothenuse. When attributing other values to n and replacing it in the previous equations, the lines when n is constant are obtained.

1.4. Novelty and Aim of This Work

As previously explained, the role of a combustion process is vital to increasing the efficiency of domestic or industrial stoves and, subsequently, the sustainability of the process, reducing the amounts of pollutants released into the atmosphere, depending on factors such as biomass composition [21,22], previous conditions [23], stove design (including its evolution to improve performance) [24–26], or burning conditions [27–29]. Thus, some studies have previously dealt with this subject, as can be observed in Table 1. These efforts focused on evolved pollutants applied to the use of domestic or industrial stoves, or simulations [30], in addition to focusing on variables such as the kind of biomass, biomass load, or pre-treatments, like wood washing or drying [31].

Table 1. Recent works related to the subject of this research.

Authors	Details and Findings	Reference
Maxwell et al.	Analysis of the emissions of three different biomass products, and their torrefied counterparts, in a domestic wood stove. After torrefaction, lower emissions (CO and CH_4) were found.	[32]
Prapas et al.	Study of the influence of a chimney on the combustion characteristics of a stove, observing changes in CO production.	[33]
Sungur et al.	Optimization of the effects of burner pot design by changing supply airflow position in a pellet stove through machine learning.	[34]

Table 1. *Cont.*

Authors	Details and Findings	Reference
Schmidt et al.	Influence of wood washing on emissions during wood combustion in a domestic pellet stove, with an observed decrease in pollutants.	[35]
Vicente et al.	Wood combustion experiments were carried out to determine the effects of different factors, like biomass load.	[36]
Toscano et al.	Combustion tests were carried out, simulating domestic utilization conditions of a pellet stove. Higher emissions (for instance, CO) were found in the steady state condition.	[37]

In that sense, the novelty of this work lies in the optimization of a pellet stove, considering both the raw materials and parameters utilized, depending on the stove's power type. Thus, an adapted optimization of a specific stove for each kind of biomass is offered, as well as an assessment of the influence of raw material on combustion optimization. Considering the above, in more detail, the aim of this work was to carry out the optimization of the combustion process in a commercial stove. For that purpose, different kinds of fuels were used at different air ratios and power levels, followed by assessing efficiency according to the flue gas flow and composition.

2. Materials and Methods

2.1. Facilities, Raw Materials, and Their Characterization

This work was carried out in the Department of Applied Physics of the Engineering School at the University of Extremadura, and consisted of the optimization study of a biomass combustion stove, using a commercial biomass stove and working at 10 Pa and 5 kW, operating with different fuels such as pine, poplar, and plum tree pellets provided by CICYTEX (Centro de Investigaciones Científicas y Tecnológicas de Extremadura). Thus, through experimental studies, the performance of this stove was optimized according to the raw material, feeding ratio, and power.

The samples were collected and homogenized to avoid considerable statistical errors due to heterogeneity, and 1–2 g of sample was prepared for each characterization. The determinations that were carried out are summarized in Table 2:

Table 2. Raw material characterization, including details according to international standards.

Parameter	Details
Proximate analysis	Biomass composition with regards to ash, moisture, volatile content, and fixed carbon.
Ash content	The solid waste after incineration. High-quality fuels present low ash content. Determination according to UNE 32004:1984 standard [38].
Moisture content	High moisture reduces energy potential, as some energy will be used to evaporate and remove moisture. According to UNE 32001:1981 standard [39].
Volatile matter	Weight loss of a fuel during heating in the absence of oxygen (apart from moisture content). According to UNE 32019:1984 standard [40].
Fixed carbon	Obtained according to the previous values, as follows: Fixed carbon = 100 − (% ash + % moisture + % volatile matter).
Ultimate analysis	The qualitative and quantitative determination of certain chemical elements, such as C, H, N, S and O, mainly.

2.2. Combustion System and Equipment

The main components of the combustion process were as follows (see Figures 4 and 5):

- Pellet stove, where the different biomass pellets were fed to carry out their combustion at different feed ratios and power.
- Gas analyzer for the combustion flue gas (Testo 335), placed in the chimney once to analyze the main components included in the combustion exhaust gas, such as O_2, CO_2, or CO. Also, an excess air coefficient (λ), which will be compared to the calculated excess air coefficient (n) in further sections, is provided using the gas analyzer.
- Temperature probe for flue gas.
- Temperature probe for inlet air.

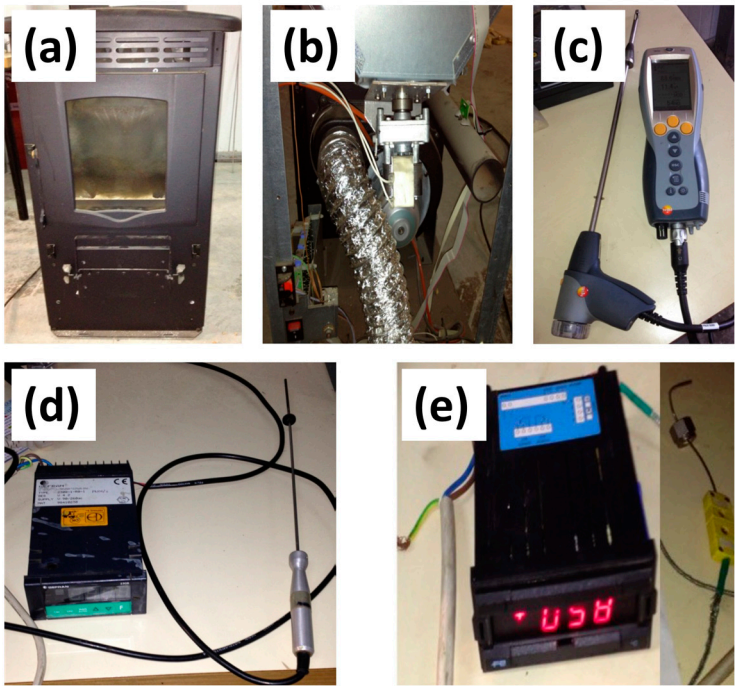

Figure 4. Main components of the biomass stove, including: (**a**) stove (front view); (**b**) stove (back view); (**c**) gas analyzer (Testo 335); (**d**) temperature probe for the exhaust gases; (**e**) temperature probe for the air supply.

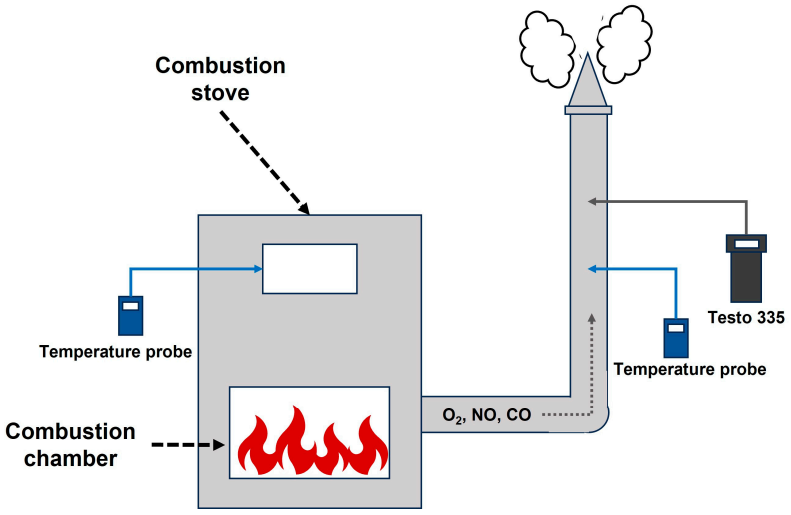

Figure 5. Schematic diagram of the combustion system.

Regarding the pellet stove (Isabella), it presented the following characteristics (included in Table 3):

Table 3. Main characteristics of the combustion stove.

Parameter	Result
Weight, kg	110
Height, mm	864
Width, mm	453
Depth, mm	497
Flue gas pipe diameter, mm	80
Air suction pipe diameter, mm	50
Maximum heating volume, m^3	115
Maximum thermal power, kW	5.8
Maximum useful thermal power, kW	5.0
Minimum useful thermal power, kW	2.5
Maximum hourly fuel consumption, kg/h	1.2
Minimum hourly fuel consumption, kg/h	0.6
Tank capacity, kg	11
Nominal electric power, W	300
Recommended flue gas pressure, Pa	10
Flue gas pressure at maximum thermal power, Pa	12
Flue gas pressure at minimum thermal power, Pa	10

Thus, Figure 4a,b show the abovementioned stove. Regarding the gas analyzer (Testo 335), it is a portable analyzer specifically used for combustion gas analysis, and measures room temperature and outlet temperature (°C), oxygen (%), NO (ppm) and CO (ppm) and calculates some parameters from these data, such as the excess air coefficient (n), thermal efficiency (η), and loss through sensitive enthalpy in the flue gas (q_a). The temperature probe for the exhaust gases (Figure 4d), which indicates temperature values in °C, was connected to a digital display. Finally, the temperature probe for inlet gas (Figure 4e), which also expresses temperature in °C, was also connected to a digital display.

Finally, Figure 5 shows the arrangement of the abovementioned components in the experimental facility and serves as a guide for the experimental procedure explained in the following subsection. Thus, as recommended in the literature, sampling of these kind of pollutants (CO, CO_2, NO_x, etc.) was carried out using gaseous analyzers placed in the chimney after combustion took place [41]. The orientation of the sampling tube was perpendicular of the gas flow, and the utilized inlet sampling procedure was based on a flange which can be opened during the sampling procedure.

2.3. Experimental Procedure

In this subsection, the main steps carried out during combustion, which are the main steps through which to obtain the Ostwald diagram (an essential tool through which to assess the results obtained in this combustion chamber), are explained according to experimental data.

First, the fuel hopper was filled with the corresponding biomass (pine, poplar, or plum tree pellets). Afterwards, the stove was switched on, and the primary fan started working. After 2 min, the worm screw started feeding the combustion chamber with pellets, and once the ignition started, combustion took place. It should be noted that the stove needed a constant pellet feed to avoid an automatic shutdown. Once the flame was generated in the biomass, the stove started to work, and the secondary fan started working after 2 min, starting the heat release from the front part of the combustion stove. The steady state was achieved after approximately 90 min, depending on the position or level selected, and then another test was carried out after changing the kind of pellet or other parameter. The measurements taken with the Testo analyzer were carried out by placing the probe in the flue gas pipe, as can be observed in Figure 5. The different conditions that were selected

for pellet combustion are included in Table 4, where different raw materials, levels, and feed ratios were used to assess their effect on combustion stove performance. As can be observed in this table, five different levels can be used in this stove, with increasing feeding rates and primary fan power levels. A selection of these combustion conditions will be discussed in the Section 3.

Table 4. The main conditions selected for pellet combustion.

Raw Material	Position or Level Selected	Pellet Feed
Pine Poplar Plum tree	1, 2, 3, 4 and 5	Normal (100%) Extra (125%)

2.4. Ostwald Diagram

In this section, the calculation of the Ostwald triangle is shown in detail (providing, as an example, the case of poplar pellet combustion, with the rest of the fuels showing equivalent behavior) as a complementary tool, in addition to the equipment used for the combustion system. Thus, the complete combustion line, the air line (n = 1), the air lines at different η values (1.5, 2, etc.), and the lines at constant CO values are explained.

Regarding the complete combustion line, Table 5 shows the points obtained in the case of poplar pellet combustion. As observed, V_{CO_2} values are obtained from Equation (9). The slope determination of complete combustion line (m_{ccl}) is obtained by using a line passing through two selected points (X_1, Y_1) and (X_2, Y_2). For that purpose, a and b parameters are determined, where a is the slope of the line and b is the independent term (see Equations (12) and (13)).

$$m_{ccl} = a = \frac{Y_1 - Y_2}{X_1 - X_2} \tag{12}$$

$$b = Y_1 - \left(\frac{Y_1 - Y_2}{X_1 - X_2}\right) X_1 \tag{13}$$

Table 5. Points on the complete combustion line for poplar pellets.

V_{O_2}, % (X)	V_{CO_2}, % (Y)	V_{O_2}, % (X)	V_{CO_2}, % (Y)
0.00	0.161	0.11	0.077
0.01	0.153	0.12	0.069
0.02	0.145	0.13	0.061
0.03	0.138	0.14	0.054
0.04	0.130	0.15	0.046
0.05	0.122	0.16	0.038
0.06	0.115	0.17	0.031
0.07	0.107	0.18	0.023
0.08	0.099	0.19	0.015
0.09	0.092	0.20	0.008
0.10	0.084	0.21	0.000

In this case, two points from Table 5 were selected—(0.00, 0.16) and (0.21, 0.00)—and used to obtain the corresponding values for m_{ccl} (that is, a)—(−0.765) and *b* (0.1607)—according to the abovementioned equations. Figure 6 shows the resulting complete combustion line for poplar pellets.

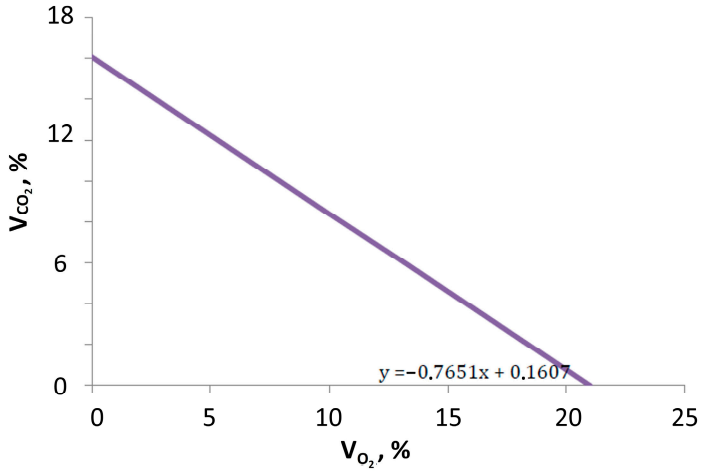

Figure 6. The complete combustion line for poplar pellets.

Regarding the air line (n = 1), the burnt gas ratio (x) was obtained using Equation (6). The selected points used to build the air line were as follows:

- V_{CO_2max}, V_{O_2} = 0, with n = 1 and x = 1. V_{CO_2max} was obtained from Equation (10), resulting in a value of 0.161.
- V_{CO_2} = 0, V_{O_2max}, with n = 1 and x = 1. V_{O_2max} was obtained from Equation (11), resulting in a value of 0.074.

From these points, (0.000, 0.161) and (0.074, 0.000), the equation of the air line can be obtained, that is, a = −2.16 (in this case, the slope when n = 1, $m_{n=1}$) and b = 0.161. The resulting line is shown in Figure 7.

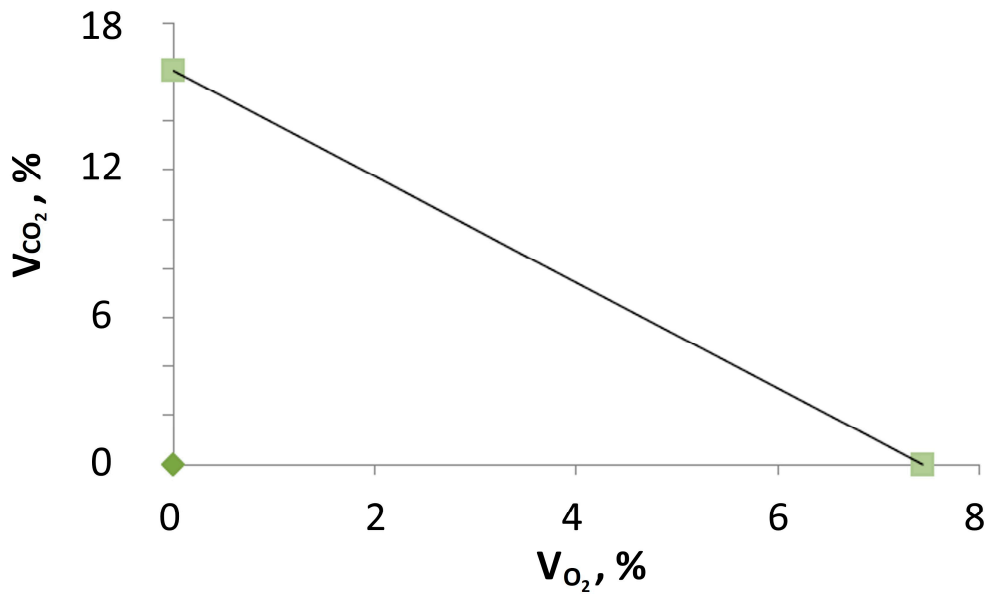

Figure 7. The air line for poplar pellet combustion.

Concerning different values of n (for instance, n = 1.5) for the air line, the elements used included the slope obtained for the air line, with n = 1.0 (that is, $m_{n=1}$); the point V_{O_2max}; $V_{CO_2=0}$; and the conditions (n = 1.5 and x = 0). The following points were obtained: (0.119, 0.000) and (0.000, 0.257). Thus, the resulting line is shown in Figure 8, as follows:

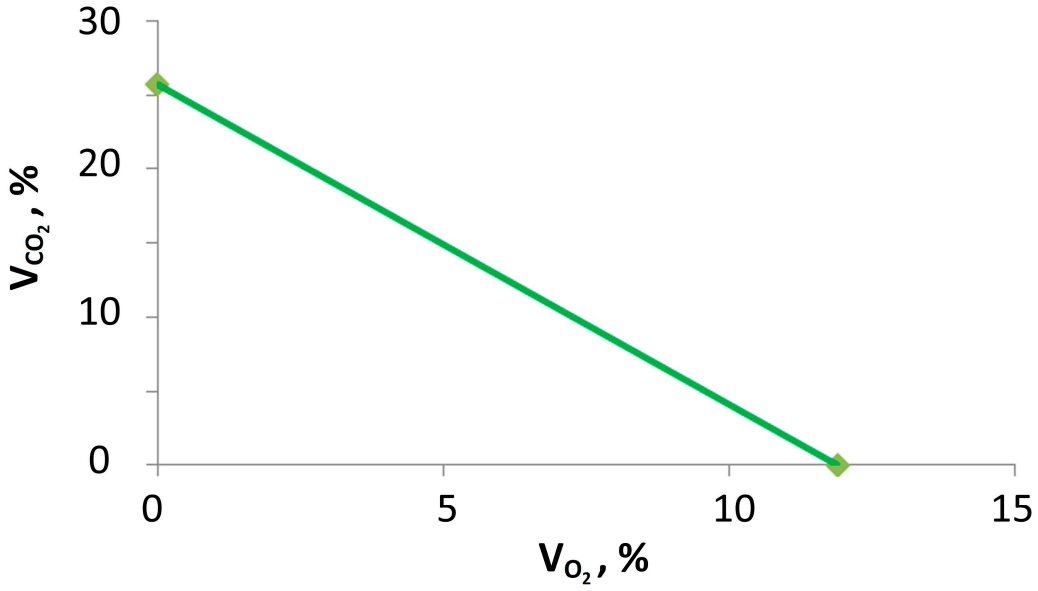

Figure 8. The air line (η = 1.5) for poplar pellets.

Concerning constant CO lines, they were obtained when a fixed value of CO was selected. For instance, in the case of CO = 0.02, the intersection point between the air line (n = 1) and the line where O_2 is constant was obtained, and then the line resulting from the abovementioned point and the slope of complete combustion was obtained. Figure 9 shows all of the lines obtained at constant values of CO (0.2, 0.4, 0.6, etc.).

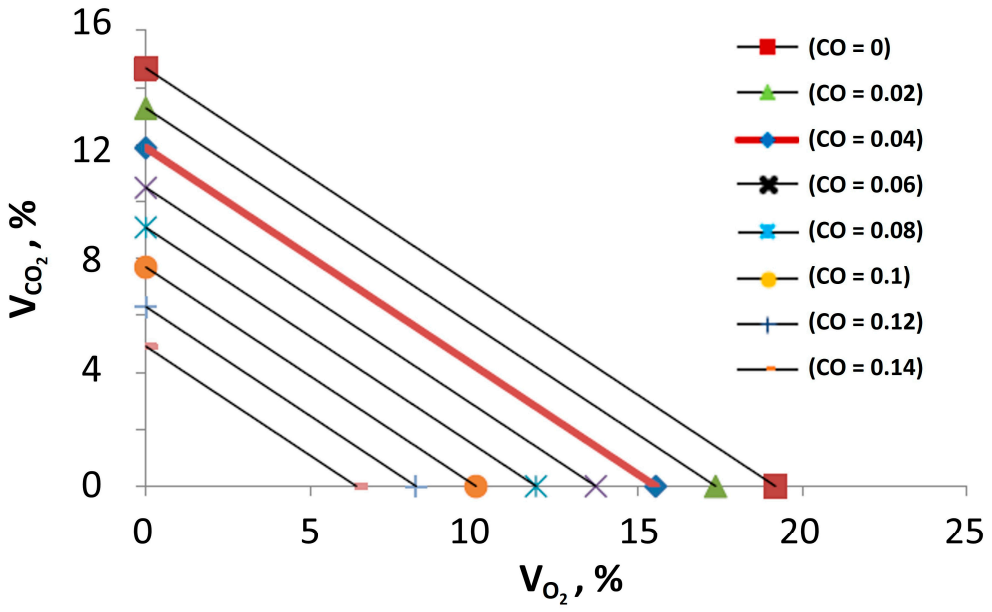

Figure 9. CO lines when CO = constant for poplar pellets.

Finally, the Ostwald diagram resulting from the abovementioned calculations, in the case of poplar pellet combustion, is included in Figure 10.

This tool is essential to checking the state of the combustion process in a selected stove, in order to assess the optimization of combustion by using different fuels, working levels, and pellet feed.

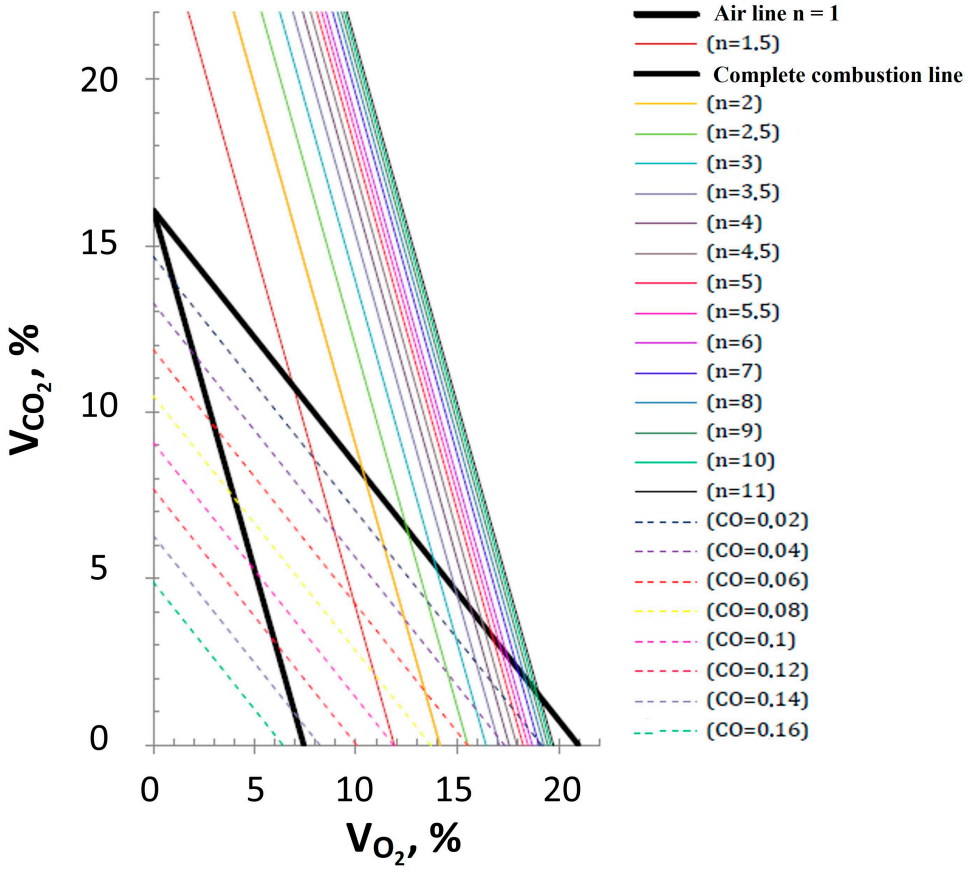

Figure 10. Ostwald diagram for poplar pellet combustion.

3. Results and Discussion

3.1. Pellet Characterization and Experiments Selected for Combustion Tests

The main results found for the pine, poplar, and plum tree pellets are included in Table 6, as follows:

Table 6. Pellet characterization.

Proximate Analysis (Dry Basis)				
Sample	Ash, %	Moisture, %	Volatile matter, %	Fixed carbon, %
Pine	0.50	6.42	84.01	15.49
Poplar	1.79	6.61	78.24	13.36
Plum tree	0.83	6.90	78.37	13.90
Ultimate analysis (Dry Basis)				
Sample	C, %	H, %	N, %	S, %	O, %
Pine	47.70	6.12	0.33	0.004	45.85
Poplar	46.40	6.01	0.52	0.028	47.04
Plum tree	47.50	6.23	0.38	0.093	45.80

These results are consistent with those of other wood pellets found in the literature, which were in the same order of magnitude [22,42]. Consequently, it can be concluded that the quality of these pellets, according to both the proximate and ultimate analyses, is standard compared to the literature. Specifically, it can be seen that the highest ash content was found in poplar pellets, the percentage of which was within the normal range found in the literature for pellets obtained from similar species. On the contrary, pine pellets offered the lowest ash content, a property which is desirable in combustion chambers. The HHVs for pine, poplar, and plum tree pellets were 4771, 4714, and 4679 kcal/kg, respectively.

For each fuel and level included in the stove (from 1 to 5), a test was carried out. Each test included 20 analyses, took 5 min long, and was conducted using the Testo 335 gas analyzer and other two temperature probes. Regarding the feeding rate, two different experiments were carried out, one with a normal feed and the other with 25% extra feed, by reducing the excess air coefficient and obtaining different results for each fuel and level. The standard biomass is labeled as "biomass I", and the increased feeding rate is referred to as "biomass II". As a result, for each experiment with a specific level and feed, the samples were labeled as follows: P (number of level) (number of feed). For instance, P2I would correspond to an experiment with the second level at a standard feeding.

For the discussion of the results, the tests with the same kind of fuel were prepared, as each fuel type showed different results regarding proximate and ultimate analyses, and, therefore, the Ostwald diagram will be different for each case (see Table 7). The aim of these comparisons was to assess the trends observed for these tests when level and feed are varied.

Table 7. The tested levels and feed ratios for each fuel.

Pine	Poplar	Plum Tree
P1I vs. P5I	P3I vs. P5I	P2I vs. P4I
P1I vs. P5II	P3I vs. P5II	P2I vs. P4II
P1II vs. P5II	P3II vs. P5II	P2II vs. P4II
P5I vs. P5II	P5I vs. P5II	P4I vs. P4II

Also, there are some parameters that were theoretically calculated. Thus, the theoretical values, n_{th} (Equation (14)), x_{th} (Equation (15)), and y_{th} (Equation (16)) differed from those obtained with the analyzer, in the fact that the former considered data from the studied fuel, whereas those obtained with the Testo analyzer did not regard the kind of fuel utilized. The following equation was used to express the excess air coefficient calculated from the data obtained from the tests and the data measured with the analyzer for a specific fuel:

$$n_{th} = \frac{-21\left(-2P_C - 6P_H + P_C V_{CO} + 6P_H V_{O_2}\right)}{\left(P_C + 3P_H\right)\left(42 + 79V_{CO} - 200V_{O_2}\right)} \quad (14)$$

In the same way, the burned gas ratio is expressed as follows:

$$x_{th} = \frac{-\left(-42P_C + 121P_C V_{CO} + 474P_H V_{CO} + 200P_C V_{O_2}\right.}{P_C\left(42 + 79V_{CO} - 200V_{O_2}\right)} \quad (15)$$

These expressions were determined through the simplification of Equations (11) and (12), used to obtain the air line (n = 1). To determine y_{th}, that is, % V_{CO_2}, similar steps included in the obtention of lines when CO was constant were followed. The difference is in point three, where:

$$y = m_{ccl} \cdot \%O_2 + b_s \quad (16)$$

In this case, x is the $\%O_2$ value obtained through the gas meter for a given fuel. Therefore, V_{CO_2}, obtained theoretically, was obtained through the following expression (Equation (17)), which was used in the tests carried out in this experiment.

$$y = V_{CO_2} = V_{O_2} \cdot m_{Rcc} + m_{n=1}\left(\frac{V_{CO}}{2}\right) + b_{n=1} - m_{Rcc}\left(\frac{V_{CO}}{2}\right) \quad (17)$$

Thus, the results obtained using these equations are included in following sections. It should be noted that y and $\%CO_2$ are different, as the former is obtained with the Ostwald diagram whereas the latter is obtained with the gas analyzer, although both refer to the same concept, that is, carbon dioxide content.

3.2. Pine Pellet Combustion

Table 8 and Figures 11 and 12 show the main results obtained for pine pellet combustion in our commercial stove when different levels were selected.

Table 8. Comparison between P1 and P5 for pine pellet combustion.

	P1		P5	
Parameter	**Average**	**Average Deviation**	**Average**	**Average Deviation**
O_2, %	18	0.01	14.8	0.006
Air supply temperature, °C	46.7	1.9	68.4	0.4
Flue gas temperature, °C	74.7	0.5	107	0.3
Ambient temperature, °C	20.9	0.6	20.5	0.2
CO, ppm	700.1	214.1	445.2	126.4
CO, %	0.070	0.021	0.045	0.013
y, %	2.27	0.46	4.75	0.44
CO_2, %	2.93	0.58	6.12	0.56
λ	7.19	1.38	3.36	0.29
η, %	85.82	3.00	89.74	0.78
qA, %	14.18	3.00	10.26	0.78
NO, ppm	17.9	6.7	43.2	6.0
Calculated n	6.94	1.33	3.26	0.28
X (x = [V_{CO_2}/(V_{CO_2} + V_{CO})])	0.966	0.016	0.991	0.002

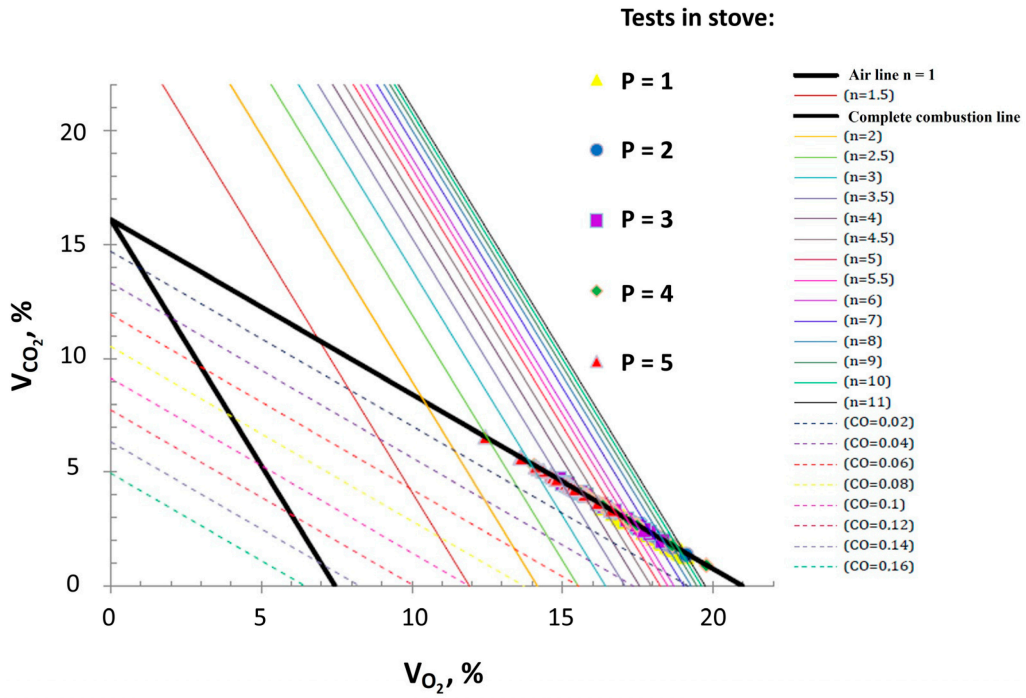

Figure 11. Ostwald diagram for pine pellets, and experimental results for each level used in the combustion stove (standard feed).

From these data, it can be inferred that a decrease in the excess air coefficient (n) was found; additionally, the total flue gas volume was reduced, which implies a decrease in losses due to sensitive enthalpy of exhaust gas (q_a), increasing thermal efficiency (η). This behavior is in accordance with the posited theory.

On the other hand, when the excess air coefficient decreased, the percentage of carbon monoxide was reduced, increasing the gas ratio that was burned (x), as well as the percentage of carbon dioxide, which implies a decrease in loss due to unburned gas, while equally increasing the thermal efficiency of the process (η). It should be pointed out that CO emissions from biomass combustion could be influenced by three factors: gas temperature, oxygen concentration, and fuel–oxygen mixing. More oxygen would result in

either a reduced gas temperature or additional residence time for a well-mixed combustion. Consequently, the design of the stove plays an important role in providing enough air during the combustion process [43]. Previous studies pointed out the requirement of a suitable air supply, while trying to avoid high airflow rates to reduce CO emissions [42]. Results showed that, if x is increased, combustion is more complete, thus decreasing loss due to unburned gas, but it is contradictory compared to the yield–loss graph and an excess air coefficient, where low values of n would imply an increase in losses due to unburned gas. Similar trends were observed with air distribution in a wood stove (with an increase in CO emissions with higher air supply ratios) [44].

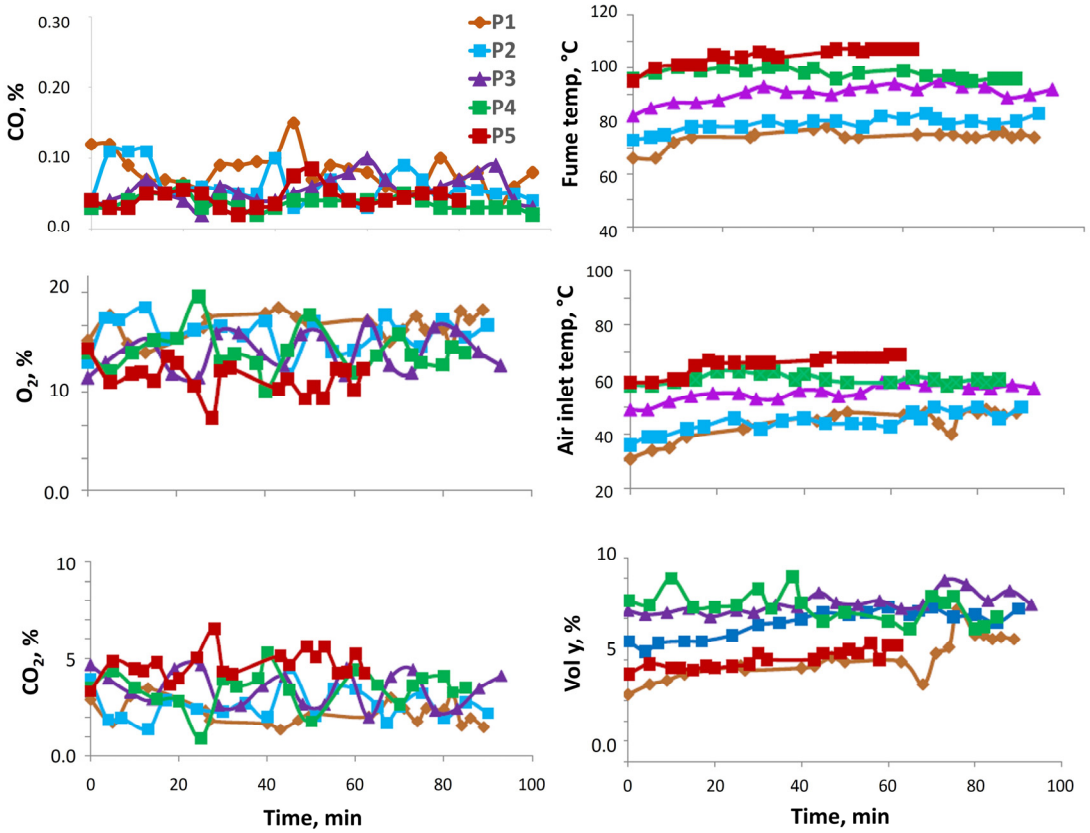

Figure 12. Evolution of main parameters for pine pellet combustion.

The outlet temperature (flue gas temperature, Figure 12), considerably increased from Position 1 to Position 5, which indicates an increase in losses due to sensitive enthalpy, as observed in previous studies for increasing input levels or positions (from 6 to 12 kW) [34]. Consequently, the yield of the process was reduced. Nevertheless, in this case, the yield increased, due to the reduction in the excess air coefficient, decreasing the total volume of flue gas and the losses due to sensitive enthalpy. In this way, the yield was improved. In other words, there are two opposite effects, whereby the decrease in flue gas volume is more important than the increase in flue gas temperature when it comes to yield determination.

The room temperature was kept practically constant during the different experiments, and there was an increase in NO content with power, as observed in Table 8, even though this increase could be considered negligeable due to the low concentration of this pollutant.

Finally, the inlet air temperature increased with power (see Figure 12), which does not necessarily imply an increase in yield, as the inlet air temperature is directly related to the useful power. Thus, paying attention to the yield concept, if there is a similar air flow, an increase in inlet air temperature would mean an increase in yield, but, in this case, the excess air coefficient decreased. Therefore, this parameter is not a determinant

in yield calculations. An increase in inlet temperature is interesting if the stove's working conditions are optimal.

The average deviation indicates that the measurements obtained in this work have been correctly taken, proving the homogeneity of the sampling process. Table 9 shows a comparison between two different combustion conditions for pine pellets. Thus, P1 with standard biomass feeding and P5 with 25% extra feeding were compared. The abovementioned differences are clearer in this example, proving that combustion was more efficient when 25% extra was fed. In other words, when experimental data are located on the left of the Ostwald diagram, the conditions would be more suitable for this combustion stove and the use of pine pellets as a fuel.

Table 9. Comparison of different levels (or positions) and feeding ratios for pine pellets (examples for P = 1, 100% feed, and P = 5, 125% feed). Down and up arrows indicate a decrease or increase in a certain parameter when P and feed were increased.

Test Parameter	Pine Pellets (P = 1, 100% Feed)	Pine Pellets (P = 5, 125% Feed)	Comparison
O_2, %	18	11.9	↓
Air supply temperature, °C	46.7	90.6	↑↑↑
Flue gas temperature, °C	74.7	113.1	↑↑↑
Ambient temperature, °C	20.9	20.8	Constant
CO, ppm	700.1	364.4	↓↓
CO, %	0.070	0.036	↓↓
y, %	2.27	6.96	↑↑
CO_2, %	2.93	8.96	↑↑
λ	7.19	2.29	↓↓↓
η, %	85.82	92.34	↑↑
qA, %	14.18	7.66	↓↓
NO, ppm	17.9	65.1	Negligible
Calculated n	6.94	2.24	↓↓
x (x = [V_{CO_2}/(V_{CO_2} + V_{CO})])	0.966	0.995	↑

Regarding different feed rations when the same power was selected (in this case, P5, as observed in Figure 13), higher increases in air inlet and exhaust gas temperatures, as well as in carbon dioxide percentage, was found in the case of 125% feed. After 30 min, these parameters stabilized, as observed in the literature for similar facilities (where gas composition and energy output achieved stability 20 min after ignition) [45]. The disproportionate increase in CO_2 emissions could be due to an increase in the air inlet for 125% feed, which could have contributed to speeding up combustion in the stove.

3.3. Plum Tree Pellet Combustion

Concerning plum tree pellets, the main results are included in Table 10 (in which Position 2 and Position 4 were selected) and Figures 14 and 15. Similar trends were observed compared with pine pellets, except for CO emissions (see Figure 15), whose values presented a constant trend in general, as observed in previous studies during the stable combustion of biomass in a commercial boiler [46].

Table 10. Comparison between P2 and P4 for plum tree pellet combustion.

	P2		P4	
Parameter	**Average**	**Average Deviation**	**Average**	**Average Deviation**
O_2, %	18.9	0.4	18.0	0.7
Air supply temperature, °C	43.6	0.7	52	0.4
Flue gas temperature, °C	69.2	0.6	90.2	1.1
Ambient temperature, °C	18.8	0.4	18.7	0.5
CO, ppm	1378.0	240.8	1372.6	533.1
CO, %	0.138	0.024	0.137	0.053
y, %	1.50	0.35	2.22	0.57
CO_2,%	1.98	0.45	2.91	0.73

Table 10. *Cont.*

	P2		P4	
Parameter	**Average**	**Average Deviation**	**Average**	**Average Deviation**
λ	10.05	1.92	7.06	1.46
η, %	79.98	4.42	81.26	4.69
qA, %	20.02	4.42	18.74	4.69
NO, ppm	40	11.2	61.4	12.9
Calculated n	9.72	1.87	6.82	1.42
X (x = [V_{CO_2} /(V_{CO_2} + V_{CO})])	0.908	0.029	0.932	0.038

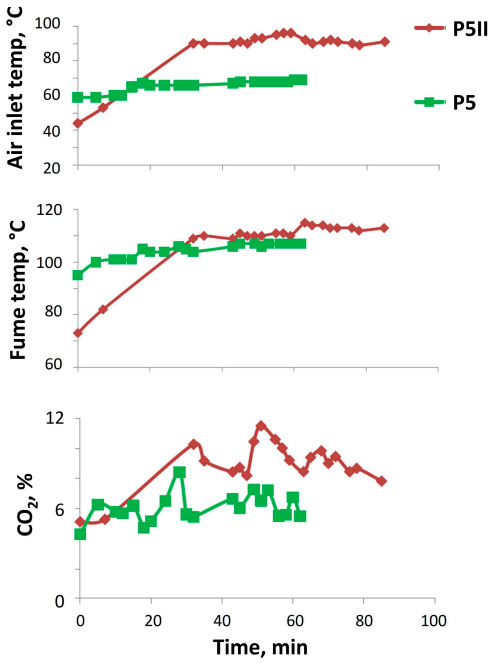

Figure 13. Comparison between different feeding rates in the case of pine pellets.

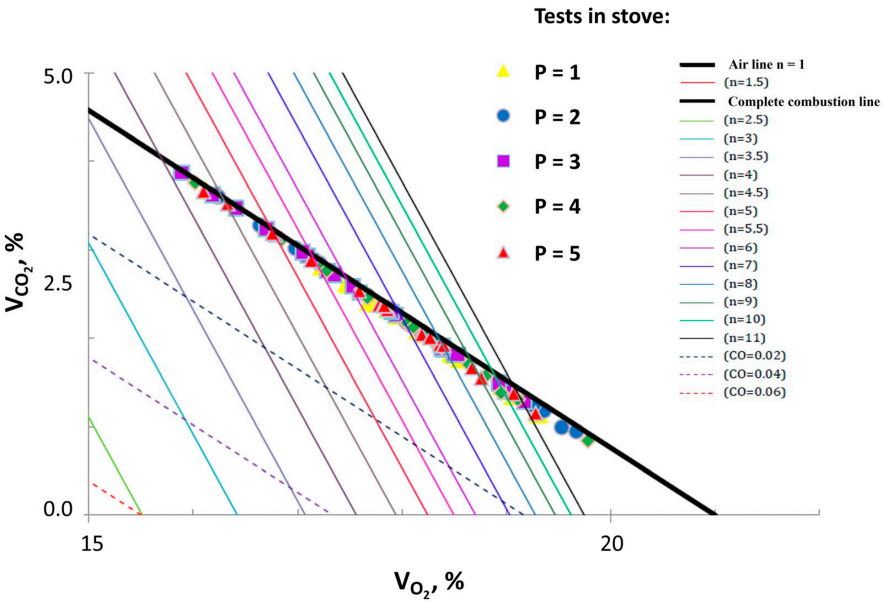

Figure 14. Ostwald diagram for plum tree pellets, and experimental results for each level used in the combustion stove.

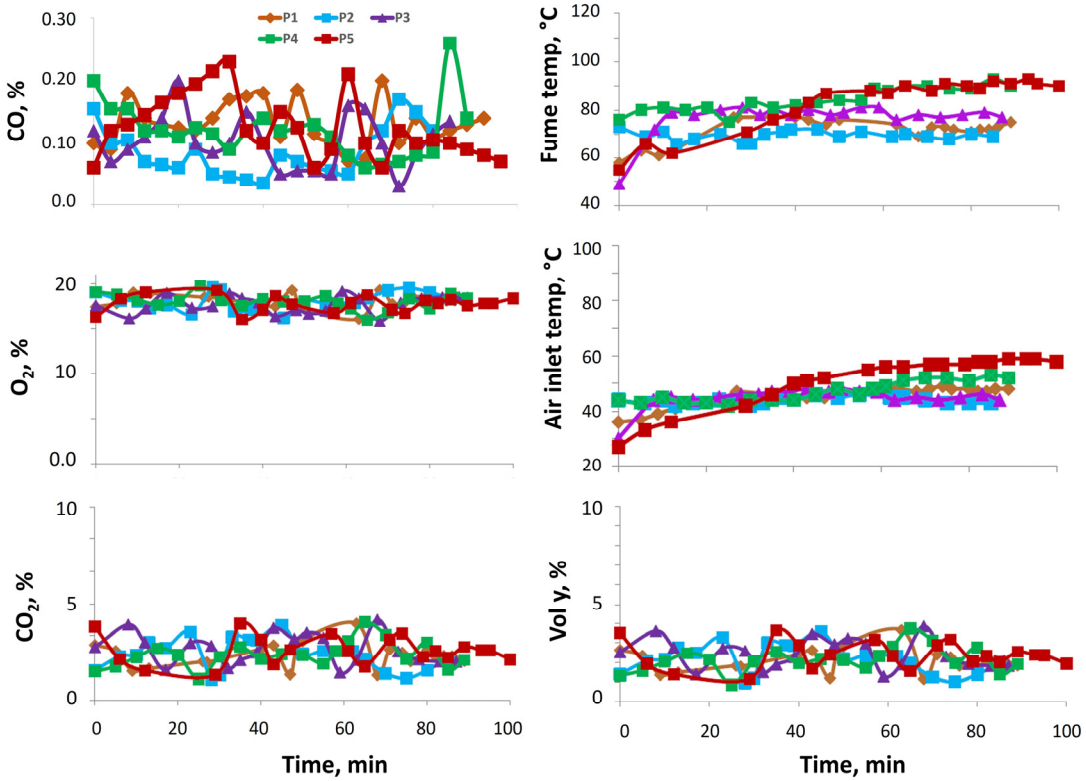

Figure 15. Evolution of main parameters for plum tree pellet combustion.

Regarding the comparison of different levels and feeding ratios for plum tree pellets, the main results are observed in Table 11. It can be observed that, when the extreme cases were compared, there were considerable differences, which were more noticeable in this case with regard to the examples selected for pine pellets. Thus, it can be seen more clearly that the stove works under more optimal conditions when extra feed is selected for plum tree pellets.

Table 11. Comparison of different levels and feeding ratios for plum tree pellets (examples for P = 2, 100% feed, and P = 4, 125% feed). Down and up arrows indicate a decrease or increase in a certain parameter when P and feed were increased.

Test Parameter	Plum Tree Pellets (P = 2, 100% Feed)	Plum Tree Pellets (P = 4, 125% Feed)	Comparison
O_2, %	18.9	14.1	↓
Air supply temperature, °C	43.6	49.1	↑
Flue gas temperature, °C	69.2	91.7	↑↑
Ambient temperature, °C	18.8	18.9	Constant
CO, ppm	1378	329.3	↓↓↓
CO, %	0.138	0.033	↓↓
y, %	1.50	5.26	↑↑
CO_2, %	1.98	6.71	↑↑
λ	10.05	3.01	↓↓↓
η, %	79.98	91.53	↑↑
qA, %	20.02	8.41	↓↓
NO, ppm	40	115.9	Negligible
Calculated n	9.72	2.92	↓↓
x (x = $[V_{CO_2}/(V_{CO_2} + V_{CO})]$)	0.908	0.994	↑

In addition, when different feed rates were compared for the same level (see Figure 16), differences with pine pellets could be found, with negligible differences in air inlet and exhaust gas temperatures, whereas the CO_2 percentage was higher with 125% feed.

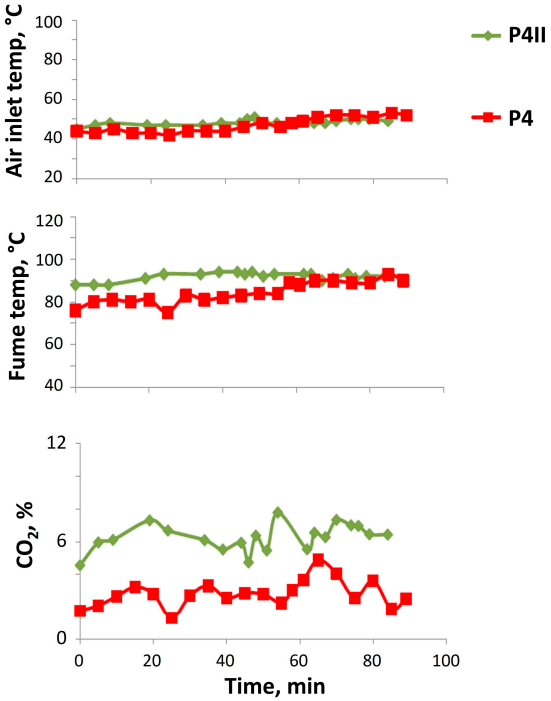

Figure 16. Comparison between different feeding rates in the case of plum tree pellets.

3.4. Poplar Pellet Combustion

Regarding Poplar pellets and their combustion performance in the domestic stove, the main results for different power levels are included in Table 12 and Figures 17 and 18. As observed, when power was increased, the excess air coefficient (η) decreased. However, unlike pine and plum tree pellets, the burned gas ratio (x) was kept practically constant regardless the level or position selected, thus increasing the flue gas temperature and, subsequently, keeping the yield of the process constant. These results are consistent, as η did not decrease as much as it did in the two previous cases, not considerably decreasing the exhaust gas total volume. In contrast, the exhaust gas temperature increased in this case (see Figure 18). This fact indicates that losses due to sensible heat are practically constant and, considering the constant trend observed for x, this implied a constant yield throughout the experiment.

Table 12. Comparison between P3 and P5 for poplar pellet combustion.

	P3		P5	
Parameter	**Average**	**Average Deviation**	**Average**	**Average Deviation**
O_2, %	17.1	1.1	16.6	0.6
Air supply temperature, °C	60.7	1.0	58.8	1.1
Flue gas temperature, °C	78.8	1.2	96.6	1.3
Ambient temperature, °C	14.2	0.5	18.9	0.5
CO, ppm	806.7	182.4	1047.1	158.5
CO, %	0.081	0.018	0.105	0.016
y, %	2.90	0.85	3.28	0.45
CO_2,%	3.76	1.09	4.26	0.57
λ	5.76	1.33	4.77	0.61
η, %	85.62	3.46	85.47	1.85
qA, %	14.38	3.46	14.57	1.85
NO, ppm	73.7	15.6	114.7	13.6
Calculated n	5.56	1.28	4.62	0.58
x (x = [V_{CO_2}/(V_{CO_2} + V_{CO})])	0.969	0.012	0.968	0.009

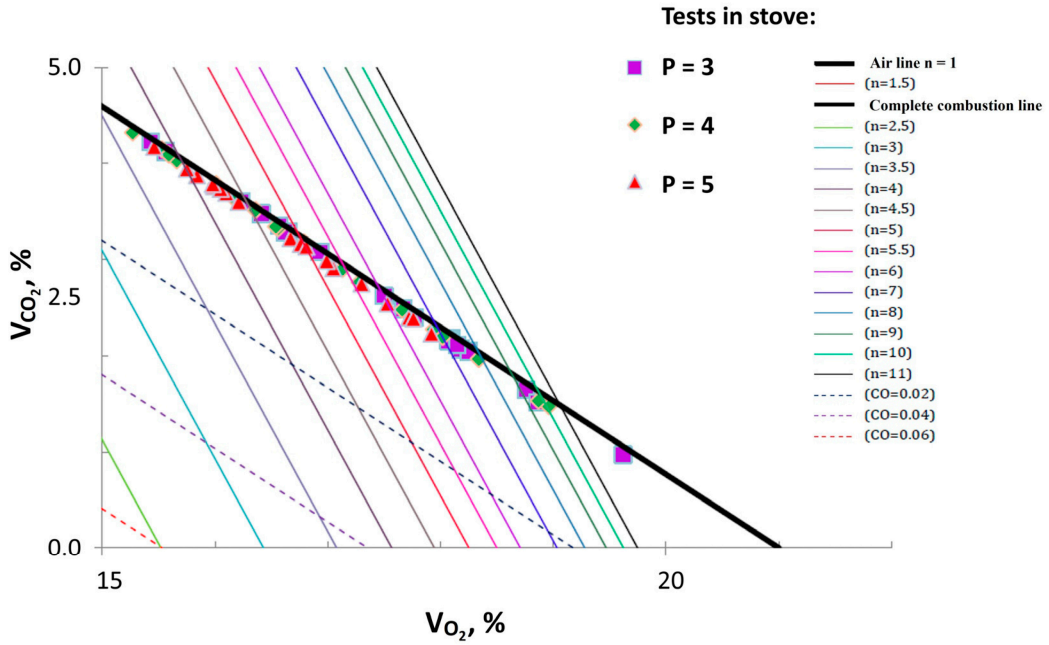

Figure 17. Ostwald diagram for poplar pellets, and experimental results for each level used in the combustion stove.

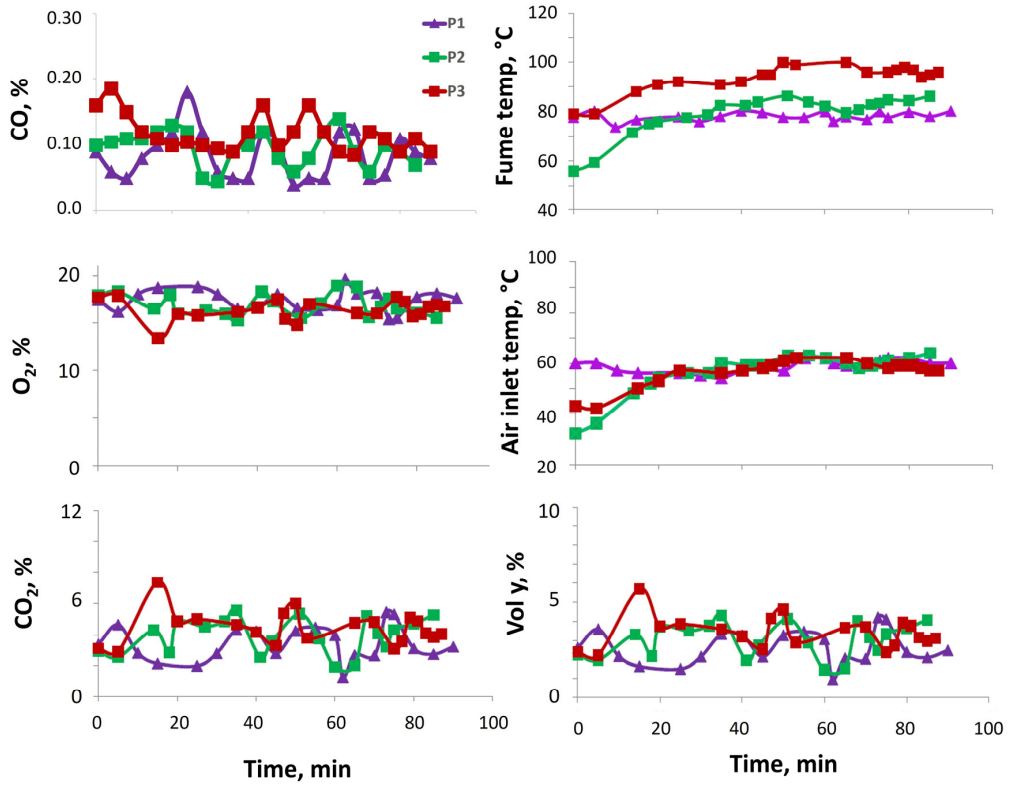

Figure 18. Evolution of the main parameters for poplar pellet combustion.

When extreme conditions were compared (see Table 13), the same trends were observed, as in the case of pine and plum tree pellets, leading to the conclusion that a decrease in excess air implied a more optimal combustion condition. Higher carbon dioxide emissions are related to higher temperatures in combustion processes, requiring temperature control according to previous studies, in which analyses of the combustion emissions of sugarcane bagasse were carried out in a burner pilot [47].

Table 13. Comparison of different levels and feeding ratios for poplar pellets (example for P = 3, 100% feed, and P = 5, 125% feed). Down and up arrows indicate a decrease or increase in a certain parameter when P and feed were increased.

Test Parameter	Poplar Pellet (P = 3, 100% Feed)	Poplar Pellet (P = 5, 125% Feed)	Comparison
O_2, %	17.1	12.5	↓
Air supply temperature, °C	60.7	77	↑
Flue gas temperature, °C	78.8	115.6	↑↑
Ambient temperature, °C	14.2	21	↑
CO, ppm	806.7	1058.6	Constant
CO, %	0.081	0.106	Constant
y, %	2.90	6.40	↑↑
CO_2, %	3.76	8.28	↑↑
λ	5.76	2.45	↓↓↓
η, %	85.62	90.53	↑
qA, %	14.38	9.47	↓↓
NO, ppm	73.7	165.4	Negligible
Calculated n	5.56	2.39	↓
x (x = [V_{CO_2}/(V_{CO_2} + V_{CO})])	0.969	0.984	↑

Finally, according to Figure 19, increasing the feeding rate showed similar results compared to the previously tested pellets, although a constant CO percentage, along with a lower increase in exhaust gas temperature when the pellet feed was at 125%, implied a higher yield for poplar pellet combustion. It should be noted that the behaviors of different kinds of biomass could be different in some aspects, such as carbon monoxide or carbon dioxide emissions, depending on their composition and disposition (raw, briquette, or pellet) [22,28,48].

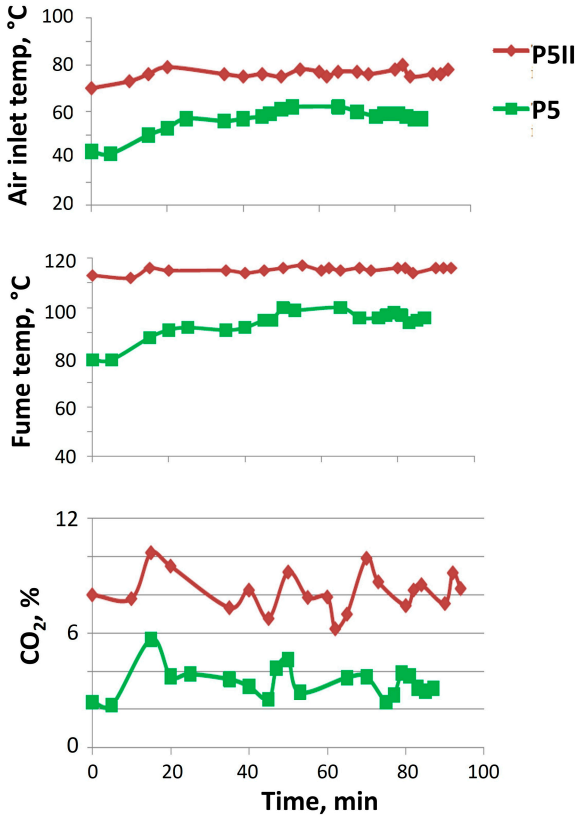

Figure 19. Comparison between different feeding rates in the case of poplar pellets.

If the different biomass products are compared at their optimum conditions (that is, P = 5 and +125% biomass for pine; P = 4 and +125% biomass for plum tree; and P = 3

and +125% biomass for poplar), interesting results can be found, like the higher carbon dioxide emission for pine pellets (8.96% on average, although similar to poplar, with 8.28%, and higher than plum tree, with 6.71%), whereas the exhaust gas temperature was similar (113.1 °C) to that of poplar pellets (115.6 °C), with a lower value for plum tree pellets (91.7 °C). Therefore, these results point out the need for adjusting the operating conditions of the stove depending on the nature of the utilized biomass products, which offer different results due to their different compositions and the differences found for the required combustion conditions.

4. Conclusions

The main findings that can be inferred from the results of this research work were as follows:

In general, when power increased, combustion was more efficient, except with poplar pellets. When the pellet feed flow increased, combustion was more efficient, with a particularly positive effect with plum tree pellets. Carbon monoxide emissions were reduced, whereas inlet air and exhaust gas temperatures increased with power, except with poplar pellets.

- Combustion was more complete when power and feed increased, decreasing energy loss except with poplar pellets. Regarding pine and plum tree pellets, thermal efficiency increased with a rise in pellet feed and power, as opposed to poplar pellets, for which this efficiency improved by modifying excess air.
- Some solutions to losses were proposed, such as sample homogenization to make the feeding rate more stable, a reduction in the excess air coefficient, and the implementation of an economizer (to reduce the exhaust gas temperature, which is a good step from both environmental and economic points of view).
- The optimum combustion conditions for pine pellets were obtained by selecting Position 5 and +25% biomass feed, with the highest yield, 92.34%, obtained with an excess air coefficient of 2.23, a burned gas ratio of 0.994, and flue gas and inlet air temperatures of 113.14 °C and 90.57 °C, respectively. Regarding plum tree pellets, Position 4 and +25% biomass feed were the optimum conditions, with the highest yield, 91.58%, obtained with an excess air coefficient of 2.91, a burned gas ratio of 0.993, and flue gas and inlet air temperatures of 91.71 °C and 49.14 °C, respectively. For poplar pellets, these conditions were P = 3 and +25% biomass supply, with the highest yield, 91.1%, obtained with an excess air coefficient of 3.18, and flue gas and inlet air temperatures of 87.66 °C and 84.66 °C, respectively.
- For this combustion chamber, it can be concluded that the three fuels studied are suitable for this facility in order to achieve optimum conditions, that is, an efficient combustion process, not showing considerable differences among the products to be selected as the ideal biomass for this experiment.

Author Contributions: Conceptualization, J.F.G. and A.Á.M.; methodology, J.F.G. and A.Á.M.; validation, J.F.G. and A.Á.M.; formal analysis, A.Á.M. and D.D.G.; investigation, A.Á.M. and D.D.G.; resources, J.F.G.; data curation, A.Á.M. and S.N.-D.; writing—original draft preparation, A.Á.M., D.D.G. and S.N.-D.; writing—review and editing, J.F.G. and S.N.-D.; visualization, J.F.G., A.Á.M. and S.N.-D.; supervision, J.F.G. and A.Á.M.; project administration, J.F.G.; funding acquisition, J.F.G. and A.Á.M. All authors have read and agreed to the published version of the manuscript.

Funding: This research received no external funding.

Institutional Review Board Statement: Not applicable.

Informed Consent Statement: Not applicable.

Data Availability Statement: Data is contained within the article.

Acknowledgments: The authors would like to thank CICYTEX for providing the raw materials for this experiment.

Conflicts of Interest: The authors declare no conflict of interest. The funders had no role in the design of the study; in the collection, analyses, or interpretation of data; in the writing of the manuscript; or in the decision to publish the results.

Nomenclature

Symbol	Meaning
CO_2	Carbon dioxide content in fumes measured with the gas analyzer
λ	Excess air coefficient directly obtained with the gas analyzer
n	Excess air coefficient
η	Thermal efficiency
qA	Loss through sensitive enthalpy in flue gas
m_{ccl}	Slope of complete combustion line
LHV	Low heating value
x	Burned gas ratio
y	Theoretical carbon dioxide content in fumes according to Ostwald diagram

References

1. Högselius, P.; Kaijser, A. Energy Dependence in Historical Perspective: The Geopolitics of Smaller Nations. *Energy Policy* **2019**, *127*, 438–444. [CrossRef]
2. Vakulchuk, R.; Overland, I.; Scholten, D. Renewable Energy and Geopolitics: A Review. *Renew. Sustain. Energy Rev.* **2020**, *122*, 109547. [CrossRef]
3. Bricout, A.; Slade, R.; Staffell, I.; Halttunen, K. From the Geopolitics of Oil and Gas to the Geopolitics of the Energy Transition: Is There a Role for European Supermajors? *Energy Res. Soc. Sci.* **2022**, *88*, 102634. [CrossRef]
4. Scholten, D.; Bosman, R. The Geopolitics of Renewables; Exploring the Political Implications of Renewable Energy Systems. *Technol. Forecast. Soc. Chang.* **2016**, *103*, 273–283. [CrossRef]
5. Carfora, A.; Pansini, R.V.; Scandurra, G. Energy Dependence, Renewable Energy Generation and Import Demand: Are EU Countries Resilient? *Renew. Energy* **2022**, *195*, 1262–1274. [CrossRef]
6. UN Sustainable Development Goals. Available online: https://www.un.org/sustainabledevelopment/ (accessed on 29 July 2023).
7. Singh, A.; Christensen, T.; Panoutsou, C. Policy Review for Biomass Value Chains in the European Bioeconomy. *Glob. Transit.* **2021**, *3*, 13–42. [CrossRef]
8. Vitoussia, T.; Leyssens, G.; Trouvé, G.; Brillard, A.; Kemajou, A.; Njeugna, E.; Brilhac, J.F. Analysis of the Combustion of Pellets Made with Three Cameroonian Biomass in a Domestic Pellet Stove. *Fuel* **2020**, *276*, 118105. [CrossRef]
9. Bioenergy Europe Wood Pellet Production Worldwide from 2000 to 2018. Available online: https://www.statista.com/statistics/509075/global-wood-pellet-production/ (accessed on 18 September 2023).
10. EurObserv'ER Solid Biomass Primary Energy Production in the European Union 2000–2021. Available online: https://www.statista.com/statistics/799329/solid-biomass-energy-production-european-union-eu/ (accessed on 18 September 2023).
11. Federal Network Agency Number of Biomass Power Plants in Germany from 2011 to 2022. Available online: https://www.statista.com/statistics/457781/biomass-plants-in-germany/ (accessed on 18 September 2023).
12. Energy Information Administration Electricity Generation from Biomass and Waste in Africa from 2000 to 2020. Available online: https://www.statista.com/statistics/1276088/electricity-generation-from-biomass-and-waste-in-africa/ (accessed on 18 September 2023).
13. EurObserv'ER Biomass Energy Production and Consumption in Finland 2015–2016. Available online: https://www.statista.com/statistics/799434/solid-biomass-production-consumption-finland/ (accessed on 18 September 2023).
14. EurObserv'ER Biomass Energy Production and Consumption in Sweden 2016–2021. Available online: https://www.statista.com/statistics/799426/solid-biomass-production-consumption-sweden/ (accessed on 18 September 2023).
15. EurObserv'ER Biomass Energy Production and Consumption in Portugal 2016–2021. Available online: https://www.statista.com/statistics/799491/solid-biomass-production-consumption-portugal/ (accessed on 18 September 2023).
16. EurObserv'ER Biomass Energy Production and Consumption in Italy 2016–2018. Available online: https://www.statista.com/statistics/799429/solid-biomass-production-consumption-italy/ (accessed on 18 September 2023).
17. EurObserv'ER Biomass Energy Production and Consumption in Spain 2015–2021. Available online: https://www.statista.com/statistics/799448/solid-biomass-production-consumption-spain/ (accessed on 18 September 2023).
18. Moayedi, H.; Aghel, B.; Abdullahi, M.M.; Nguyen, H.; Safuan A Rashid, A. Applications of Rice Husk Ash as Green and Sustainable Biomass. *J. Clean. Prod.* **2019**, *237*, 117851. [CrossRef]
19. Lewandowski, W.M.; Ryms, M.; Kosakowski, W. Thermal Biomass Conversion: A Review. *Processes* **2020**, *8*, 516. [CrossRef]

20. Hustad, J.E.; Wnju, O.K. Biomass Combustion in IEA Countries. *Biomass Bioenergy* **1992**, *2*, 239–261. [CrossRef]
21. Oladosu, K.O.; Babalola, S.A.; Kareem, M.W.; Ajimotokan, H.A.; Kolawole, M.Y.; Issa, W.A.; Olawore, A.S.; Ponle, E.A. Optimization of Fuel Briquette Made from Bi-Composite Biomass for Domestic Heating Applications. *Sci. Afr.* **2023**, *21*, e01824. [CrossRef]
22. Pokhrel, R.P.; Gordon, J.; Fiddler, M.N.; Bililign, S. Determination of Emission Factors of Pollutants From Biomass Burning of African Fuels in Laboratory Measurements. *J. Geophys. Res. Atmos.* **2021**, *126*, e2021JD034731. [CrossRef]
23. Labbé, R.; Paczkowski, S.; Knappe, V.; Russ, M.; Wöhler, M.; Pelz, S. Effect of Feedstock Particle Size Distribution and Feedstock Moisture Content on Pellet Production Efficiency, Pellet Quality, Transport and Combustion Emissions. *Fuel* **2020**, *263*, 116662. [CrossRef]
24. Brandelet, B.; Rose, C.; Landreau, J.; Druette, L.; Rogaume, Y. Toward a Cleaner Domestic Wood Heating by the Optimization of Firewood Stoves? *J. Clean. Prod.* **2021**, *325*, 129338. [CrossRef]
25. Han, J.; Liu, X.; Hu, S.; Zhang, N.; Wang, J.; Liang, B. Optimization of Decoupling Combustion Characteristics of Coal Briquettes and Biomass Pellets in Household Stoves. *Chin. J. Chem. Eng.* **2023**, *59*, 182–192. [CrossRef]
26. Shaisundaram, V.S.; Chandrasekaran, M.; Sujith, S.; Praveen Kumar, K.J.; Shanmugam, M. Design and Analysis of Novel Biomass Stove. In *Materials Today: Proceedings*; Elsevier Ltd.: Amsterdam, The Netherlands, 2020; Volume 46, pp. 4054–4058.
27. Zhang, H.; Zhang, X.; Wang, Y.; Bai, P.; Hayakawa, K.; Zhang, L.; Tang, N. Characteristics and Influencing Factors of Polycyclic Aromatic Hydrocarbons Emitted from Open Burning and Stove Burning of Biomass: A Brief Review. *Int. J. Environ. Res. Public Health* **2022**, *19*, 3944. [CrossRef]
28. Qi, J.; Liu, L.; Wu, J. Improving Combustion Technology for Cooking Activities for Pollutant Emission Reduction and Carbon Neutrality. *Atmosphere* **2022**, *13*, 561. [CrossRef]
29. Huang, Y.; Partha, D.B.; Harper, K.; Heyes, C. Impacts of Global Solid Biofuel Stove Emissions on Ambient Air Quality and Human Health. *Geohealth* **2021**, *5*, e2020GH000362. [CrossRef]
30. Lustenberger, D.; Strassburg, J.; Strebel, T.; Mangold, F.; Griffin, T. Simulation Tool for the Development of a Staged Combustion Pellet Stove Controller. *Energies* **2022**, *15*, 6969. [CrossRef]
31. Al-Kassir, A.; Coelho, P.; García-Sanz-Calcedo, J.; Moral, F.J.; Al-Karany, R.K.; Yusaf, T. An Experimental Technology of Drying and Clean Combustion of Biomass Residues. *Appl. Sci.* **2018**, *8*, 905. [CrossRef]
32. Maxwell, D.; Gudka, B.A.; Jones, J.M.; Williams, A. Emissions from the Combustion of Torrefied and Raw Biomass Fuels in a Domestic Heating Stove. *Fuel Process. Technol.* **2020**, *199*, 106266. [CrossRef]
33. Prapas, J.; Baumgardner, M.E.; Marchese, A.J.; Willson, B.; DeFoort, M. Influence of Chimneys on Combustion Characteristics of Buoyantly Driven Biomass Stoves. *Energy Sustain. Dev.* **2014**, *23*, 286–293. [CrossRef]
34. Sungur, B.; Basar, C.; Kaleli, A. Multi-Objective Optimisation of the Emission Parameters and Efficiency of Pellet Stove at Different Supply Airflow Positions Based on Machine Learning Approach. *Energy* **2023**, *278*, 127896. [CrossRef]
35. Schmidt, G.; Trouvé, G.; Leyssens, G.; Schönnenbeck, C.; Genevray, P.; Cazier, F.; Dewaele, D.; Vandenbilcke, C.; Faivre, E.; Denance, Y.; et al. Wood Washing: Influence on Gaseous and Particulate Emissions during Wood Combustion in a Domestic Pellet Stove. *Fuel Process. Technol.* **2018**, *174*, 104–117. [CrossRef]
36. Vicente, E.D.; Duarte, M.A.; Calvo, A.I.; Nunes, T.F.; Tarelho, L.; Alves, C.A. Emission of Carbon Monoxide, Total Hydrocarbons and Particulate Matter during Wood Combustion in a Stove Operating under Distinct Conditions. *Fuel Process. Technol.* **2015**, *131*, 182–192. [CrossRef]
37. Toscano, G.; Duca, D.; Amato, A.; Pizzi, A. Emission from Realistic Utilization of Wood Pellet Stove. *Energy* **2014**, *68*, 644–650. [CrossRef]
38. *UNE 32004:1984*; Solid Mineral Fuels. Determination of Ash. UNE Normalización Española: Madrid, Spain, 1984.
39. *UNE 32001:1981*; Hard Coal and Anthracite. Determination of Total Moisture. UNE Normalización Española: Madrid, Spain, 1981.
40. *UNE 32019:1984*; Hard Coal and Coke. Determination of Volatile Matter Content. UNE Normalización Española: Madrid, Spain, 1984.
41. Yao, W.; Zhao, Y.; Chen, R.; Wang, M.; Song, W.; Yu, D. Emissions of Toxic Substances from Biomass Burning: A Review of Methods and Technical Influencing Factors. *Processes* **2023**, *11*, 853. [CrossRef]
42. Deng, M.; Li, P.; Shan, M.; Yang, X. Optimizing Supply Airflow and Its Distribution between Primary and Secondary Air in a Forced-Draft Biomass Pellet Stove. *Environ. Res.* **2020**, *184*, 109301. [CrossRef]
43. Zhang, Y.; Zhang, Z.; Zhou, Y.; Dong, R. The Influences of Various Testing Conditions on the Evaluation of Household Biomass Pellet Fuel Combustion. *Energies* **2018**, *11*, 1131. [CrossRef]
44. Holubčík, M.; Čajová Kantová, N.; Jandačka, J.; Čaja, A. The Performance and Emission Parameters Based on the Redistribution of the Amount of Combustion Air of the Wood Stove. *Processes* **2022**, *10*, 1570. [CrossRef]
45. Wang, X.; Niu, B.; Deng, S.; Liu, Y.; Tan, H. Optimization Study on Air Distribution of an Actual Agriculture Up-Draft Biomass Gasification Stove. *Energy Procedia* **2014**, *61*, 2335–2338. [CrossRef]
46. Lasek, J.A.; Matuszek, K.; Hrycko, P.; Głód, K.; Li, Y.H. The Combustion of Torrefied Biomass in Commercial-Scale Domestic Boilers. *Renew. Energy* **2023**, *216*, 119065. [CrossRef]

47. Costa, M.A.M.; Schiavon, N.C.B.; Felizardo, M.P.; Souza, A.J.D.; Dussán, K.J. Emission Analysis of Sugarcane Bagasse Combustion in a Burner Pilot. *Sustain. Chem. Pharm.* **2023**, *32*, 101028. [CrossRef]
48. Kougioumtzis, M.A.; Kanaveli, I.P.; Karampinis, E.; Grammelis, P.; Kakaras, E. Combustion of Olive Tree Pruning Pellets versus Sunflower Husk Pellets at Industrial Boiler. Monitoring of Emissions and Combustion Efficiency. *Renew. Energy* **2021**, *171*, 516–525. [CrossRef]